Catena 158 (2017) 235–249

Contents lists available at ScienceDirect

Catena

journal homepage: www.elsevier.com/locate/catena

Hydro-geomorphological modelling of ash-fall pyroclastic soils for debris flow initiation and groundwater recharge in Campania (southern Italy)

Francesco Fusco, Vincenzo Allocca, Pantaleone De Vita*

Dipartimento di Scienze della Terra, dell'Ambiente e delle Risorse (DiSTAR), University of Naples Federico II, (Italy)

ARTICLE INFO

Keywords:
Ash-fall pyroclastic soil deposits
Field hydrological monitoring
Hillslope hydrology
Rainfall-induced shallow landslides
Aquifer recharge

ABSTRACT

Carbonate mountain ranges surrounding volcanic centers in the Campania region of southern Italy are covered by discontinuous ash-fall pyroclastic deposits of variable thicknesses. The cover thickness and stratigraphy are relevant to hydrological controls on both rainfall-induced landslides and groundwater recharge. To improve understanding of the hydrologic regimes within the pyroclastic soil mantle, a hydrological monitoring station was installed upslope of a debris flow source area in the Sarno Mountains. Monitoring results demonstrate consistently unsaturated conditions, strong seasonal and inter-annual variations in pressure head, and delayed and damped dynamics at different depths related to rainfall and evapotranspiration patterns. Frequencies of recorded pressure head time series were analyzed to quantify the seasonal hydrological regime of the cover as a whole, as well as variations within individual soil horizons. For the whole ash-fall pyroclastic soil cover, variable seasonal frequencies of pressure head were recognized exceeding landslide alert and groundwater recharge threshold values. Analysis of frequencies for individual soil horizons showed a strongly delayed timing determining in winter and summer an opposite hydrological behavior between the shallowest and deepest soil horizons. A model that accounts for topographic variations in cover thickness and these hydrological regimes is proposed to quantify hydro-geomorphological controls on debris flows triggering and groundwater recharge. The model is based on the estimation of ash-fall pyroclastic soil thickness along slopes by the total thickness fallen in a given area and an inverse relationship with slope angle, allowing the assessment at the distributed scale over peri-volcanic mountainous areas. Moreover, it links the spatially variable thicknesses of ash-fall pyroclastic soils to the amount of soil water storage allowing the assessment of frequency of hydrological conditions leading to debris flow initiation and groundwater recharge.

1. Introduction

The carbonate mountainous areas that surround the Campanian Plain (Campania, southern Italy) are characterized by unusual surficial geological conditions due to the covering of ash-fall pyroclastic deposits, erupted in the last 39 k-yrs. mainly by the Somma-Vesuvius volcano and subordinately by the Phlegrean Fields volcanic center. In such a geomorphological framework, the ash-fall pyroclastic soil mantle exerts a very relevant hydrological behavior, depending on spatially variable deposition and heterogeneity of stratigraphic settings. Furthermore, the existence of a dense vegetation cover living on the pyroclastic mantle is another factor to be taken into account, depending on particular hydrological properties of pyroclastic soils and climatic features. The related principal issues are recurrent rainfall-induced shallow landslides, involving pyroclastic deposits and leading to deadly debris-flows, and groundwater recharge of underlying karst aquifers as well, which are very relevant for the feeding of regional aqueduct systems (Allocca et al., 2014).

The landslide hazard along the Avella, Sarno, Salerno and Lattari mountain ranges, which surround the Campania Plain (Fig. 1) and cover an area of about 650 km^2, is a well-known national issue due to the repeated debris flows events which have caused the loss of about 900 lives since 1900. A significant advance to understand mechanisms and processes leading to instability of ash-fall pyroclastic soil covers and estimate landslide hazard was given after the high magnitude debris flow event, which occurred on 5–6 May 1998 along the Sarno Mountains and caused the loss of 160 lives. The strong cause-effect relationship between occurrence of heavy rainfall and landslide triggering led firstly to estimate Intensity-Duration (I-D) rainfall thresholds (Caine, 1980) by an empirical approach (Calcaterra et al., 2000; De Vita and Piscopo, 2002). Subsequently, also deterministic approaches, based on a coupled modelling of hydrological conditions occurring within the ash-fall pyroclastic cover during heavy rainstorms and slope stability (Lu and Godt, 2013; Bordoni et al., 2015) were attempted (Crosta and

* Corresponding author.
E-mail address: padevita@unina.it (P. De Vita).

http://dx.doi.org/10.1016/j.catena.2017.07.010
Received 18 January 2017; Received in revised form 5 July 2017; Accepted 11 July 2017

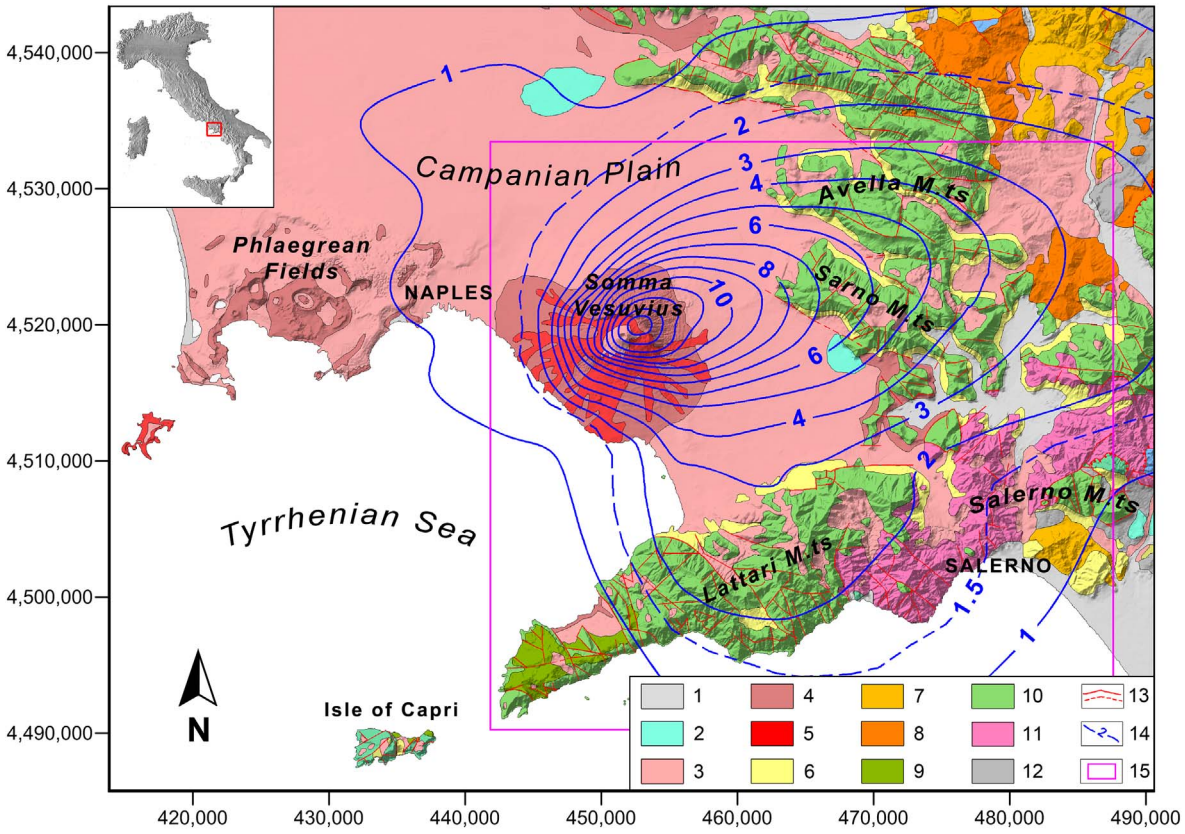

Fig. 1. Geological map of the area including mountain ranges surrounding the Somma-Vesuvius volcano: 1) alluvial deposits; 2) travertine deposits; 3) incoherent ash-fall deposits (Recent Pyroclastic Complex); 4) mainly coherent ash-flow deposits (Ancient Pyroclastic Complex); 5) lavas; 6) detritus and slope talus deposits; 7) tardo-orogenic terrigenous deposits; 8) syn-orogenic terrigenous deposits; 9) Miocene flysch; 10) Middle Jurassic-Upper Cretaceous limestone; 11) Lower Triassic-Middle Jurassic dolomites and calcareous limestone; 12) pre-orogenic basinal units; 13) outcropping and buried faults; 14) total isopachous line (meters) of ash-fall pyroclastic deposits erupted by the Plinian Somma-Vesuvius' eruptions (modified from: De Vita et al., 2006a, 2006b; De Vita and Nappi, 2013), representing z_0 value (Eq. (1)); 15) area represented in Fig. 4. Coordinates along map borders are in the UTM WGS84 system.

Dal Negro, 2003; De Vita et al., 2013; Pagano et al., 2010; Papa et al., 2013a). In these approaches, effects on slope resisting and driving forces of unsaturated (Lu and Likos, 2004) and saturated conditions (Terzaghi, 1943) were taken into account. These studies allowed both the comprehension of slope instability mechanisms, recognizing the role of stratigraphic and morphological settings on unsaturated/saturated throughflow, and the assessment of deterministic I-D rainfall thresholds. Moreover, other studies were focused on the hydrological monitoring of ash-fall pyroclastic soil mantles, which appeared an important achievement for the setting up of effective early warning systems (Damiano et al., 2012; De Vita et al., 2012; Fusco et al., 2013; Fusco and De Vita, 2015; Greco et al., 2013; Sorbino, 2005). These studies revealed a dominant unsaturated condition and a complex hydrological regime, from hourly to seasonal time scales. Given these findings another advance was carried out to assess the seasonal effect of hydrological conditions on I-D thresholds (Napolitano et al., 2016), allowing to estimate also uncertainties due to a variable antecedent hydrological status of the ash-fall pyroclastic soil mantle on rainfall conditions leading to slope instability.

In addition to the shallow landslide issue, the hydrological regime of ash-fall pyroclastic mantle plays an important role on groundwater recharge of underlying karst aquifers because determining the amounts of water losses toward the atmosphere through the evapotranspiration process and percolation down to the groundwater table. A recent study on groundwater recharge of karst aquifers of the Campania region covered by ash-fall pyroclastic soils (Allocca et al., 2015) confirmed the relevant role of these soil coverings, whose water storage determines the equivalence between actual evapotranspiration (AET) and the potential one (PET). Therefore, considering the strategic relevance of karst aquifers surrounding the Campanian Plain (Allocca et al., 2014), the understanding of hydrological behavior and regime of pyroclastic soil mantle appears another important advance for modelling groundwater recharge of these aquifers.

Considering both issues, the hydrological regime and processes taking place at different time scales within the ash-fall pyroclastic soil mantled slopes are crucial aspects to be assessed. To pursue this focus we carried out a study that can be understood in the hillslope hydrology branch (Kirkby, 1978; VV.AA., 1990, 1996). The expected results were supposed potentially fostering future assessments of both landslide hazard and groundwater recharge (Healy, 2010) of karst aquifers.

The hydrological role of the ash-fall pyroclastic soil mantle along mountain slopes surrounding the Campanian Plain is spatially variable, depending on thicknesses and stratigraphic settings. Therefore its distributed modelling is conceivable as a hydro-geomorphological model (Iida, 1999; Onda et al., 2004; Sidle and Onda, 2004), which couples the spatial distribution of ash-fall pyroclastic soil thickness and the hydrological behavior of pyroclastic soil coverings. In such a direction, results of preceding studies aimed at the spatial modelling of ash-fall pyroclastic soils thickness in the areas surrounding the volcanic centers of the Campania (De Vita et al., 2006a, 2006b; De Vita and Nappi, 2013) give the basis for the reconstruction of a hydro-geomorphological model of the ash-fall pyroclastic mantle.

In this paper we present a study on the temporal and spatial variability of the hydrological conditions of the ash-fall pyroclastic soil mantle, which are conceived as both preparatory factors for triggering landslides phenomena and controlling groundwater recharge of karst aquifers nearby the Campanian Plain. The experimental research started with the analysis of pressure head time series acquired within the whole thickness of the ash-fall pyroclastic soil mantle through a soil hydrological monitoring station, set in a representative slope area of the

Sarno Mountains. Furthermore, due to the control of the soil thickness on hydrological response dynamics of the ash-fall pyroclastic soil cover, the field monitoring outcomes were extended to a distributed scale by considering an empirical model that links thickness of the ash-fall pyroclastic soil mantle to slope angle (De Vita et al., 2006a, 2006b; De Vita and Nappi, 2013).

2. Geomorphological and hydrogeological framework

The study area is located in the Sarno Mountains which, together with the Avella, Salerno and Lattari mountain ranges, is at the border of the Campanian Plain and overlooking the Somma-Vesuvius and Phlegrean Fields volcanic centers (Fig. 1). The Sarno Mountains and the other adjoining ones are formed by Mesozoic carbonate platform series which during the Miocene compressive tectonic events were thrust over the external palaeogeographical units, characterized by oceanic basin sedimentation (D'Argenio et al., 1973; Mostardini and Merlini, 1986; Patacca and Scandone, 2007). A the end of orogenetic phase, these units were faulted during the Quaternary extensional tectonic phases, thus subsiding along the Tyrrhenian border and forming a semi-graben structure in which a back-arc volcanic activity begun in the Phlegrean Fields and Somma-Vesuvius volcanic districts, respectively since 39 k-yrs. and 25 k-yrs. B.P. Pyroclastic deposits derived by the explosive volcanic activity filled the structural depression, forming the Campanian Plain, and covered the nearby mountain ranges.

Complete volcaniclastic series can be found in the plain areas surrounding the volcanic edifices even if intercalated with fluvial or marine deposits and/or locally eroded by the palaeo-hydrographic network. In the plain area, a reference volcaniclastic series was identified nearby the footslope of the Sarno Mountains, where two principal volcaniclastic complexes were identified (Rolandi et al., 2000): the Ancient Pyroclastic Complex (APC), mainly formed by ash-flow and ash-fall deposits of the Phlegrean Fields' eruptions, and the Recent Pyroclastic Complex (RPC), comprising the Somma-Vesuvius' ash-fall deposits (Rolandi et al., 2000). Seven major Plinian eruptions were identified for the latter: Codola (25 k-yrs), Sarno (17 k-yrs), Ottaviano (8 k-yrs), Avellino (3.5 k-yrs), Pompei (79 CE), 472 CE and 1631 CE Along mountain slopes, only ash-fall deposits of the RPC can be extensively found with spatially variable thicknesses and stratigraphic settings, which are typically characterized by intercalated unweathered pumiceous lapilli and pedogenized horizons (paleosols) formed during the stages between consecutive eruptions.

Ash-fall pyroclastic soil coverings are involved frequently in rainfall-triggered, very rapid, complex landslides (sensu Cruden et al., 1996; Hungr et al., 2014; Varnes, 1978), characterized by different evolutionary stages with varying rheological behaviors and kinetic energy, related to slope morphology, thicknesses of the involved ash-fall pyroclastic soil coverings and soil water content, among the principal factors. The evolutionary model of these landslides identifies up to three consecutive stages: 1) initial debris slide (soil slip), involving a few tens of cubic meters of ash-fall pyroclastic soils; 2) debris avalanche (Hungr et al., 2014), causing the involvement of other material along the slope and a considerable increase of the landslide volume by a dynamic liquefaction mechanism; 3) debris flow (Hungr et al., 2014), when the landslide is channeled in the hydrographic network and its volume further increases by the entrainment of material along its path. The initial debris slide is always present and may evolve directly into a debris flow or limited to a debris avalanche only. It follows that landslides in the intermediate or final stages (debris avalanche and debris flow), in which they assume a typical rheology of a viscous fluid, are triggered by a small initial landslide (debris slide or soil slip), so that they can be defined as "*landslide triggered debris flow*" (Jakob and Hungr, 2005). The volume of initial shallow landslides ranges from 10^1 to 10^2 m^3, thus indicating that the susceptibility of initial landslides depends on factors, such as variations of ash-fall pyroclastic soil thickness, mechanical and hydraulic properties and variation of morphological factors, which can vary at a spatial scale comprised from 10^0 to 10^1 m.

Carbonate mountains that surround the Campanian Plain host karst aquifers of strategic relevance for the Campania region and for other adjoining regions of the southern Italy. Due to the high permeability and annual groundwater recharge of these aquifers, which favor a high specific groundwater yield (about 2.5×10^{-2} $m^3 \cdot s^{-1} \cdot km^{-2}$), a huge basal groundwater circulation exists outleting from few high-discharge basal springs. The location of the latter and the groundwater circulation pattern as well is controlled by stratigraphic and/or structural factors of the carbonate mountains.

Depending on their thicknesses and distinctive hydrological properties, ash-fall pyroclastic soil coverings exert a very relevant role on groundwater recharge and infiltration processes. The main aspect is related to the high water retention capacity of pyroclastic soils (Napolitano et al., 2016), which permits a high storage of soil water. Such a condition and climate characteristics determine mostly an energy-limited system (Budyko, 1974), in which AET and PET are equivalent, and the development of a dense vegetation formed chiefly by chestnut deciduous forests (*Castanea sativa*).

2.1. Spatial distribution of ash-fall pyroclastic soil thickness

A fundamental basis for assessing the hydrological role of ash-fall pyroclastic soils mantling slopes was the modelling of thicknesses (DeRose et al., 1991; Pelletier and Rasmussen, 2009; Catani et al., 2010) at a distributed scale over the whole peri-Vesuvian mountainous area. To achieve this goal, data and results of preceding studies (De Vita et al., 2006a; De Vita and Nappi, 2013) were considered in this research. These studies were focused on empirical modelling of ash-fall pyroclastic soils thicknesses and stratigraphic settings along slopes. A first step was the assessment, at the regional scale, of the total theoretical thickness of ash-fall pyroclastic soils by the algebraic sum of all isopach maps of principal Plinian eruptions of the Phlegrean Fields and Somma-Vesuvius volcanoes, known from the scientific literature. By this reconstruction, the distribution of the theoretical total ash-fall deposits was recognized varying heterogeneously around the volcanic vents and characterized by two main dispersal axes, the principal oriented eastward and the secondary southeastward (Fig. 1).

The total theoretical thickness values were validated by a comparison with field measurements and observations carried out along the Avella, Sarno, Lattari and Salerno mountain ranges by test pits or light dynamic penetrometer tests (De Vita and Nappi, 2013). Thickness measurements, taken along the vertical, were transformed in stratigraphic values by the projection in the plane normal to the slope and then compared with the corresponding theoretical stratigraphic values, calculated by:

$$z = z_0 \times \cos \alpha \quad (1)$$

where, z is the stratigraphic thickness, z_0 the total theoretical thickness fallen in the area (Fig. 1) and α the local slope angle.

By this comparison, the actual stratigraphic thickness of the ash-fall pyroclastic soil mantle were observed well matching with the theoretical one for slope angle values lower than 28°. Differently, for slope angle values > 28°, actual stratigraphic thicknesses were found lower than the theoretical ones fallen in the same area, with a progressive decrease as the slope angle increases, up to negligible values for slope angle values > 50°. Such a distribution model was considered chiefly controlled by landsliding, occurring mostly for slope angle values > 28° (de Riso et al., 1999) (Fig. 2). Such findings were integrated in an empirical distribution model of ash-fall pyroclastic deposits along the peri-Vesuvian mountain ranges (De Vita and Nappi, 2013) (Fig. 3).

Test pits carried out in different sites allowed reconstructing stratigraphic settings of the volcaniclastic series along slopes, whose description was based on the recognition of the principal pedogenetic horizons (USDA, 2014), lithostratigraphic features and soil classification by the USCS system.

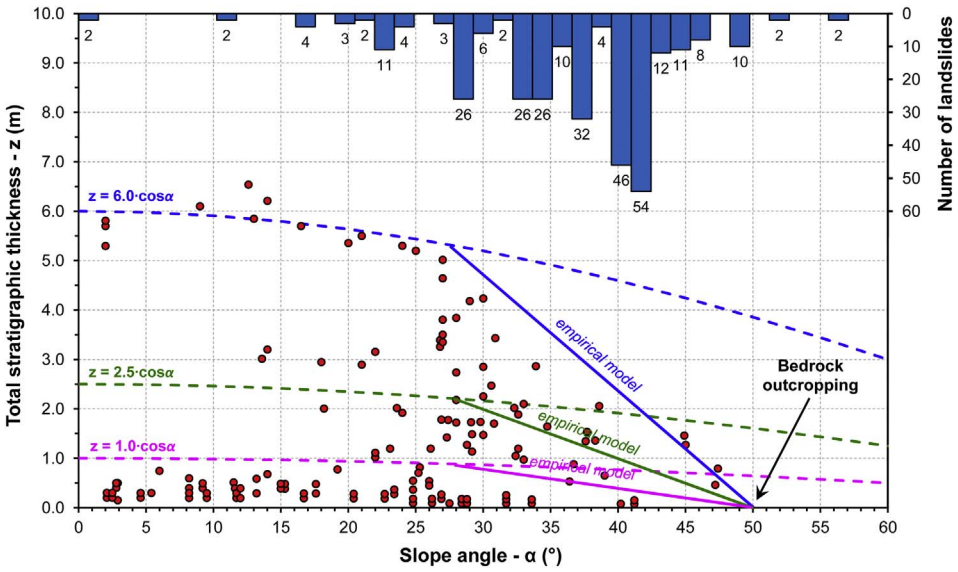

Fig. 2. Scatterplot of total stratigraphic thickness of ash-fall pyroclastic soil mantle (z), measured in sample areas, with slope angle (red dots) and comparison with theoretical models (Eq. (1)) applied for typical conditions of the Sarno (z_0 = 6.0 m; blue dashed curve), Lattari (z_0 = 2.5 m; green dashed curve), Avella and Salerno (z_0 = 1.0 m; magenta dashed curve) mountain ranges (modified from De Vita and Nappi, 2013). The theoretical models envelope field data up to slope angle of 28°. Instead, for slope angle values > 28°, field data are enveloped by linear decreasing trends (see colored straight lines) diverging from the theoretical models to the disappearance of the ash-fall pyroclastic covering for slope angle > 50°. The divergence between theoretical and actual thicknesses is due to landsliding, as it is well testified by the major frequencies of slope angle (see upper histogram) in source areas of initial debris slides (de Riso et al., 1999). (For interpretation of the references to colour in this figure legend, the reader is referred to the web version of this article.)

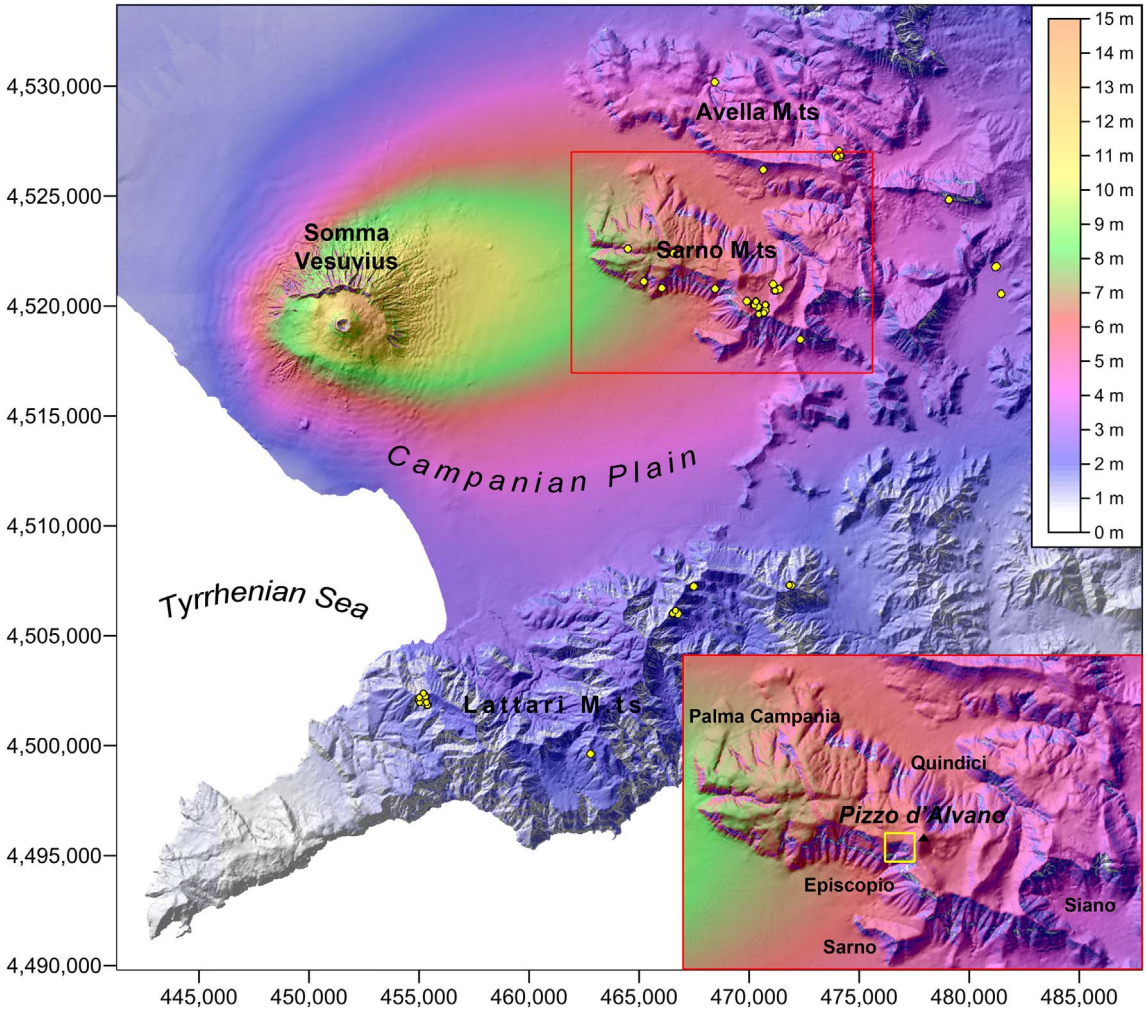

Fig. 3. Distribution model of ash-fall soil pyroclastic deposits in the area surrounding the Campanian Plain (modified after De Vita and Nappi, 2013). Values of stratigraphic thickness are expressed in meters. Sampling areas for field soil thickness measurements are also shown (yellow dots). In the lower-right box is a zoomed view of the Sarno Mountains and the approximate location of the monitoring station. Coordinates along map borders are in the UTM WGS84 system. (For interpretation of the references to colour in this figure legend, the reader is referred to the web version of this article.)

Different complete stratigraphic settings were found in morphological conservative areas (with slope angle lower than 28°), depending on the distance from the Somma-Vesuvius volcano and orientation of dispersal axes. In the conservative areas of the Sarno Mountains, complete volcaniclastic series were observed being formed, from the top, by A and B horizons (top soil), consisting of strongly weathered and pedogenised fine and coarse pumiceous ashes (SM), which overlay alternated Bb horizons, or paleosols (SM), and up to three C horizons. The latter consist of scarcely weathered pumiceous gravels, ranging from coarse ash to lapilli in grain size (GW and GP) and corresponding to deposits of CE 472, Avellino (3.6 k-yrs) (Rolandi et al., 1993b) and Ottaviano (8.0 k-yrs) (Rolandi et al., 1993a) eruptions. At the bottom of the volcaniclastic series, a basal paleosol (Bb_{basal} horizon) (SM), wrapping the carbonate bedrock and filling open discontinuities of the rock mass, was always observed. Complete volcaniclastic series were found on the Lattari Mountains being characterized by A and B horizons (topsoil) and two C horizons, ascribed respectively to deposits of 1944 (Cole and Scarpati, 2010) and CE 79 (Lirer et al., 1973) eruptions, with an intercalated Bb horizon (SM). Also in this case, a basal paleosol (Bb_{basal} horizon) covering the carbonate bedrock was constantly found. The existence of C horizons, formed by pumiceous gravels (GW and GP), at the base of B and Bb soil horizons (SM), allows the formation of capillary barrier effect during infiltration process due to the strong contrast in unsaturated hydraulic conductivity (Mancarella et al., 2012).

The thinning of the pyroclastic soil mantle for slope angle > 28°, up to its nearly disappearance for values > 50°, was recognized having a strong influence on the stratigraphic settings of the volcaniclastic series along the slopes (De Vita et al., 2006a, 2006b). The reduction of the total thickness was found determining the downslope pinching out of the pyroclastic horizons, both for C and Bb horizons, up to the direct overlying of the B horizon on the Bb_{basal} one.

Within the source areas of initial debris slides, the Bb_{basal} horizon was always observed outcropping, thus demonstrating the formation of the rupture surface within the ash-fall pyroclastic mantle. Moreover, the lack of traces of water flow emerging through the Bb_{basal} horizon seems to prove that the instability of the ash-fall pyroclastic soil covering is not caused by groundwater flow coming from the bedrock, as it was supposed in other geotechnical models (Celico et al., 1986; Cascini et al., 2008).

3. Data and methods

With the aim to understand hydrological conditions leading to rainfall-induced slope instabilities and groundwater recharge of underlying aquifers, the hydrological regime of the ash-fall pyroclastic soil mantle was studied by a monitoring station set up in a sample area located along the southwestern slope of the Mount Pizzo D'Alvano (Sarno Mountains) (Fig. 3). In detail, the monitoring station was located upslope of the source area of one of the several tens of debris flows, which in May 1998 caused 160 fatalities and destroyed many buildings and infrastructures of the Sarno, Episcopio and Quindici towns. Due to the ash-fall pyroclastic soil thickness and stratigraphic setting, as well as to morphological features and vegetation cover, we considered a sample area also representative for assessing the hydrological role of pyroclastic soil mantle on groundwater recharge of karst aquifers.

Engineering geological investigations were carried out in the study area to reconstruct in detail stratigraphic and geometric settings controlling the initial debris slide that successively evolved in a catastrophic debris flow (Fig. 4). Specifically, upslope of the landslide crown and along a rectilinear transect of 23 m length in the slope direction line, six light dynamic penetrometer tests were carried out. Moreover, to correlate dynamic penetrometer logs with the local stratigraphic setting, three exploratory pits were also executed correspondingly. Undisturbed samples were collected from test pits. Laboratory tests for soil identification (USCS), mechanical

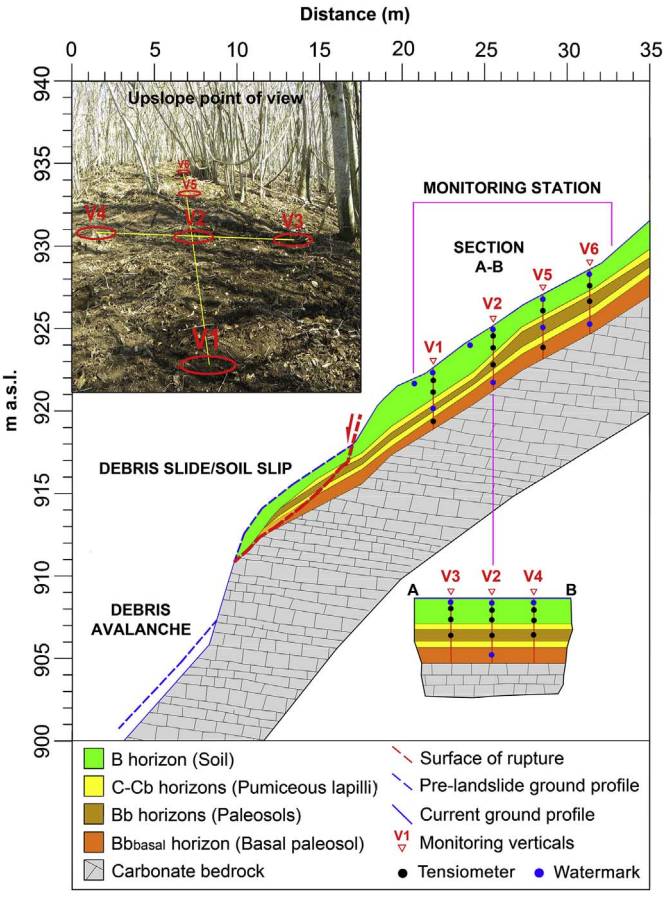

Fig. 4. Geological model of the monitoring station site reconstructed by field investigations, location of the monitoring verticals (V1-V6) and approximate position of tensiometers and Watermark sensors. In the upper-left box an upslope-oriented photo of the monitored plot is also shown.

characterization and unsaturated/saturated soil properties assessment were carried out (De Vita et al., 2013; Napolitano et al., 2016). Coupling field and laboratory tests, a detailed engineering geological model of the test area was reconstructed. Results of field investigations, already considered in a previous paper (Fusco and De Vita, 2015), show a stratigraphic series characterized by a typical alternation of paleosols and pumiceous lapilli horizons (Table 1), which matches well to the other ones detected in other areas of the peri-Vesuvian carbonate slopes.

The site of the monitoring station, upslope of the landslide main scarp, is characterized by a fairly rectilinear profile, with an average slope angle of about 32°. Instead, downslope of the main scarp, an abrupt increase of the slope angle and the outcrop of the carbonate bedrock form a rocky scarp about 5.0 m high (Fig. 4). From the landslide crown, down to the upper edge of the rocky scarp, a decrease of pyroclastic soil mantle thickness and modification of stratigraphic setting were recognized by the downslope thinning of C and Cb horizons up to their pinching out (Fig. 4).

The land cover of the sample area is characterized by a deciduous forest of chestnut (*Castanea sativa*) with sparse evergreen brushwood. This condition is common in the peri-Vesuvian mountain slopes and it can be considered recurrent for the source areas of debris flows.

Given the aim of our study, the setting of the monitoring station was designed on the basis of the local geological model and specifically focused on monitoring pressure head (h) selectively in each pyroclastic soil horizon. In situ and laboratory saturated hydraulic conductivity tests were carried out on 75 samples allowing the characterization of saturated hydraulic conductivity (K_{sat}) (Table 2). Moreover, the parameters of the van Genuchten's equation (van Genuchten, 1980) (Eq. (2))

Table 1
Stratigraphic setting of the hydrological monitoring site. The value of z0 for this area is 4.7 m (Fig. 1).

Vertical depth of the bottom (m)	Vertical thickness (m)	Lithological and lithostratigraphic descriptions USCS classification	Horizon (ID)
0.10	0.10	Humus (Pt)	A
1.30	1.20	Very loose soil of pyroclastic horizons highly subjected to pedogenetic processes with dense root apparatuses (SM). Generally dark brown colored.	B
1.60	0.30	Very loose pumiceous lapilli horizon (gravel) with low degree of weathering (GW-GP). Dark greenish gray colored. Pollena eruption (CE 472).	C
2.50	0.90	Weathered and pedogenized soil of pyroclastic origin constituted by fine to coarse ash and subordinately by pumiceous lapilli. Paleosoil (SM). Dark reddish brown colored.	Bb
2.90	0.40	Pumiceous lapilli (gravel) from very angular to angular, with maximum 6 cm of diameter, in primary deposition, matrix almost absent. Light yellowish gray colored. Avellino eruption (3.7 kyrs B.P.).	Cb
3.80	0.90	Weathered and pedogenized soil of pyroclastic origin constituted by fine to subordinate coarse ashes. Basal paleosoil (SM). Dark yellowish brown colored.	Bb_{basal}
?	?	Carbonate bedrock, weathered and fractured with open discontinuities filled by soil of the overlying horizon. Light gray colored.	R

Table 2
Range of saturated hydraulic conductivity (Ksat), between percentiles of 25% and 75%, determined for each ash-fall pyroclastic horizon (De Vita et al., 2013).

Soil horizon (USDA)	Percentile 25% < K_{sat} < Percentile 75% (m/s)	Number of samples
B	$4.82 \times 10^{-5} < K_{sat} < 1.26 \times 10^{-4}$	18
Bb	$6.00 \times 10^{-6} < K_{sat} < 2.64 \times 10^{-5}$	13
C	$2.82 \times 10^{-3} < K_{sat} < 1.26 \times 10^{-2}$	29
Bb_{basal}	$2.48 \times 10^{-7} < K_{sat} < 6.84 \times 10^{-6}$	15

Table 3
Parameters of van Genuchten's SWRC equation (De Vita et al., 2013).

Horizon	B	C	Bb	Bb_{basal}	Bedrock
θ_s [−]	0.50	0.56	0.59	0.63	0.03
θ_r [−]	0.080	0.001	0.200	0.001	0.020
α [m^{-1}]	5.60	4.20	0.73	7.20	4.31
n [−]	1.57	1.43	1.32	1.11	3.10

for the Soil Water Retention Curve (SWRC) were estimated (Table 3) by the Tempe Cells apparatus (Soilmoisture Inc.):

$$\theta(h) = \theta_r + \frac{\theta_s - \theta_r}{[1 + |\alpha/|h||^n]^m} \quad (2)$$

where, θ_s ($m^3 \cdot m^{-3}$) is the saturated volumetric water content, θ_r ($m^3 \cdot m^{-3}$) the residual volumetric water content, h (m) is soil matric pressure head, α (m^{-1}) is the inverse of the air-entry head, n (dimensionless) is the pore-size distribution parameter, and m = 1–1/n. An optimization procedure was used to fit the experimental data to Eq. (2) by means of RETC software (van Genuchten et al., 1991).

Jet Fill tensiometers (Soilmoisture Inc.) and tensiometer tubes, provided at the top by rubber septum stoppers (Soil Measurement System Inc.), were used for monitoring pressure head in the range comprised between 0.0 and about − 8.0 m at sea level. For the second type of tensiometers, measurements were made by Tensicorder (Soil Measurement System Inc.), consisting of an electronic pressure dial to be connected to the internal part of the tensiometer tube by a nylon tubing and a syringe needle puncturing the self-sealing rubber septum stopper. To measure pressure head values lower than about − 8.0 m at sea level, Watermark sensors (Irrometer, Riverside, CA) were also installed. The functioning of these sensors is based on the variable resistivity of a gypsum lamina, depending on soil water content, and it is extended over a wider range of pressure head, down to − 20.4 m.

Assuming that the highest pressure head variations occur in the shallower horizons because influenced more strongly by rainfall events and evapotranspiration process, the most of the sensors were installed in the B soil horizons (Table 4). Other sensors were distributed in the deeper Bb and Bb_{basal} horizons. No sensors were installed in the C horizon due to its coarse grain size which prevented a good hydraulic contact between soil and sensors and inhibited a reliable functioning.

Table 4
Number of sensors installed in the ash-fall pyroclastic soil mantle for pressure head monitoring for different depth zones (except for the C horizon).

Horizon	Tensiometer	Watermark	Number of sensors	Range depth (m)
B	16	8	24	0.0–1.5
Bb	5	2	7	1.8–2.5
Bbb	2	2	4	3.5–4.0

Sensors were nested in six vertical arrangements and their upper terminations, including manometers, septum stoppers and dataloggers, were enclosed in as many sealed plastic boxes, which were buried in the upper part of the B horizon for protection against environmental damaging. Vertical arrangements were set in alignment with two straight transects, respectively parallel and perpendicular to the slope direction line (Fig. 4). The one in the slope direction line, consisting of four vertical arrangements (V1, V2, V5 and V6), was set starting from the crown zone and extended upslope for a length of about 10.0 m. The second was set intersecting the first transect in the V2 vertical arrangement and with two additional ones (V3 and V4), respectively located about 5.0 m from the V2 (Fig. 4).

The monitoring period was comprised between December 2010 and December 2014 (about four years). The measurement frequency was set differently from tensiometers, not provided of automated recording, and other sensors connected to dataloggers. In the first case the reading frequency was weekly. Instead, for other sensors with automated recording, the frequency was set with a periodicity of 10–15 min. Analyses were carried out on data aggregated at the daily time scale by a respective time upscaling, based on a linear variation between two successive measurements, and downscaling, achieved by the calculation of the daily mean value.

To analyze the effect of rainfall and evapotranspiration processes on the hydrological regime of ash-fall pyroclastic coverings, daily rain and air temperature data were gathered from a meteorological station controlled by the Civil Protection Department in the nearby locality of Torriello (ID rain-gauge 15,285), located at about 0.8 km from the monitoring station site.

To understand seasonal hydrological behavior of ash-fall pyroclastic soil cover, Duration Curves (DC) of pressure head time series were reconstructed being this type of statistical analysis usually applied in hydrological sciences to study frequencies of river floods and spring discharges (Dalrymple, 1960; Helsel and Hirsch, 2002; Stedinger and Cohn, 1986; Webb and Betacourt, 1992). DC analysis was conceived as fundamental for assessing comprehensively the temporal probability (hazard) of landslide triggering, which is given by the compound

probability of assumed antecedent hydrological conditions of the ash-fall pyroclastic soil covers and of a rainfall event with certain intensity and duration values. Moreover, by the pressure head time series and SWRCs of each pyroclastic soil horizon (Table 3), water content (θ) time series were estimated. Subsequently the total Soil Water Depth stored in the ash-fall pyroclastic soil cover (SWD) was calculated (Kutilek and Nielsen, 1994) by:

$$SWD = \sum_{i=1}^{n} \theta_i \cdot z_i \quad (3)$$

where: θ_i ($m^3 \cdot m^{-3}$) corresponds to the volumetric water content for the i^{th} soil horizon; z_i (m) is the thickness of the i^{th} soil horizon; n is the number of soil horizons.

The SWD was estimated for the characteristic pressure head levels of Saturation (SAT), Field Capacity (FC) and Permanent Wilting Point (PWP), corresponding respectively to pressure values (MPa) (Kirkham, 2005), and equivalent height of water column (m), of: 0.00 MPa (0.0 m); − 0.03 MPa (− 3.06 m); − 1.50 MPa (− 153.1 m). Finally, the SWD of the Available Water Content (AWC) feeding the evapotranspiration demand was calculated as the difference between SWDs at FC and PWP levels. At this scope, annual PET was calculated by the Thornthwaite equation (Thornthwaite, 1948) by air temperature data recorded at the Torriello meteorological station.

Given, the z_0 value (Fig. 1) of the sample area, the SWD calculation was joined with the distribution model of soil mantle thickness, which varies with the slope angle (De Vita et al., 2006a; De Vita and Nappi, 2013). Such hydro-geomorphological model was considered demonstrative of all other conditions existing in the peri-Vesuvian mountainous areas, which are characterized by variable z_0 and slope angle values (Fig. 1 and Eq. (1)).

4. Results

The whole pressure head time series recorded in the four monitoring years showed a significant seasonal control (Fig. 5), characterized by pressure head values always ranging in unsaturated conditions and in different ways influenced by precipitation regime and water losses due to evapotranspiration process. Pressure head time series showed that saturated conditions were not observed in the ash-fall pyroclastic soil cover even after stronger rainfall events. Conditions of near saturation, with pressure head values around − 0.5 m, were only occasionally recorded and not exceeding upward the limit of − 0.3 m. Instead, all the soil horizons, although not in the same period, have reached, and hypothetically dropped below the detection limit of − 20.4 m (Table 5).

During the rainy periods, occurring typically from November to March, higher pressure head values were recorded, due to the combined effects of higher rainfall and lower evapotranspiration rates. In these periods, pressure head values were observed ranging between − 0.3 m and − 3.2 m. These periods were characterized by a series of peaks of pressure head corresponding to rainfall events or following them shortly (Fig. 5). The temporal correspondence between peaks of pressure head and rainfall events was observed being more direct for shallower horizons and damped and delayed for deeper ones.

During periods with snow cover, principally occurring in February, pressure head values showed that infiltration process was strongly limited to just the shallowest soil horizons. In the dry period, starting from April until October, pressure head values, after an initial exponential decrease occurring firstly in the upper part of the ash-fall pyroclastic soil cover and then moving progressively in depth, ranged between − 3.2 m and below the functioning limit of Watermark sensors (h < − 20.4 m). This behavior was related principally to the increase of evapotranspiration rate and to the decrease of rainfall events from the late spring to the early autumn. Leaf growth of deciduous chestnut forest occurring during this period was also recognized as playing a predominant role in water loss from the pyroclastic cover. Starting from September, corresponding approximately to the end of the dry period, the abrupt increase of pressure head in the upper part of the pyroclastic mantle was correlated to the occurrence of rainfall events and secondly to the stop of leaf activity. In this period, although the infiltration front was observed having a progressive deepening through shallower horizons, a further decrease of pressure head in deeper horizons was also detected (Fig. 5).

Pressure head values recorded at different depths were compared considering the periods from September to December of 2011, 2012 and 2013 (2014 was excluded due to the limited duration of recording). In these periods three hydrological stages were identified (Fig. 6). The stage 1 is representative of the beginning of the rainy season, from September to October. During this stage the values in the near surface vary widely, depending on the occurrence of intermittent rainfall events, whereas the values at greater depths are more constant. Specifically, pressure head values in the shallow subsurface (< 0.5 m depths) varied widely from the near-saturated conditions (− 0.3 m > h ≥ − 0.5 m) to very dry conditions below the functioning limit of Watermark sensors (h < − 20.4 m), depending on the recent rainfall patterns. In contrast, pressure head values at greater

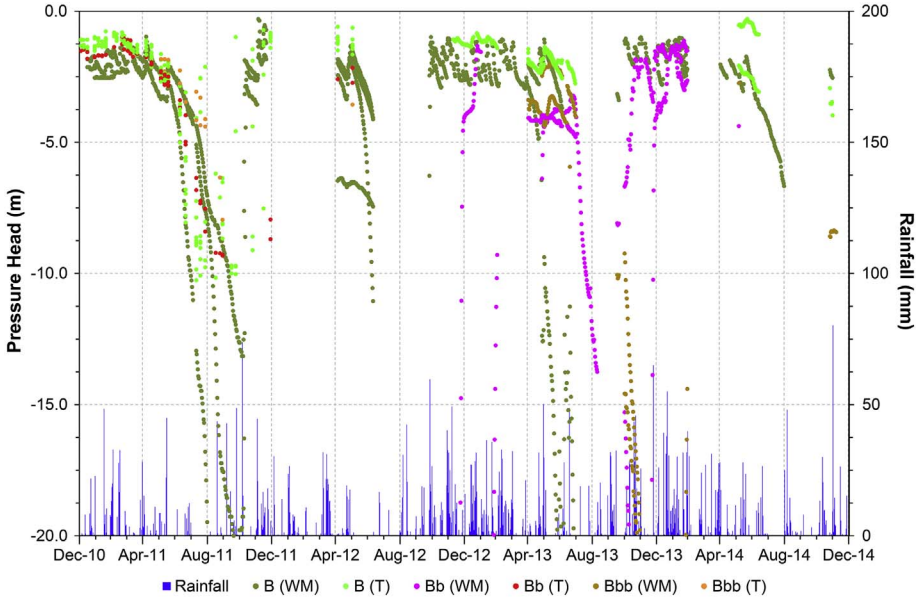

Fig. 5. Pressure head time series of mean values measured for principal pyroclastic soil horizons (B, Bb and Bb_{basal}) by means of tensiometers (T) and Watermark sensors (WM). Daily rainfall data are also shown.

Table 5
Descriptive statistics of annual pressure head values (m) recorded for each horizon.

Horizon	2011			2012			2013			2014		
	Min	Median	Max	Min	Median	Max	Min	Median	Max	Min	Median	Max
B	< −20.4	−2.5	−0.3	−11.1	−2.4	−0.6	< −20.4	−2.1	−0.8	< −20.4	−2.4	−0.3
Bb	−9.3	−2.3	−1.0	< −20.4	< −20.4	−2.2	< −20.4	−4.4	−1.3	< −20.4	−2.7	−1.1
Bb_{basal}	−8.0	−3.1	−1.8	< −20.4	< −20.4	−3.6	< −20.4	−15.7	−2.0	< −20.4	< −20.4	−2.8

depths (> 2.0 m) varied over a narrower range (between −7.0 m and −15.0 m). The stage 2 is characterized by the stabilization of the rainy period, typically occurring in November. During this period the infiltration front is uniformly formed giving near saturation conditions about down to 1.0 m of depth. Contrastingly to the wetting of the B soil horizon, a further drying of deeper Bb and Bb_{basal} soil horizons was recognized by the lowering of pressure head values down to the functioning limit of Watermark sensors (h < −20.4 m). The stage 3 corresponds to the rainy season, occurring since December, when the infiltration front reaches the Bb horizon with pressure head values varying from the near saturation to −7.0 m, down to 2.5 m of depth. In this stage, the lowest Bb_{basal} horizon still remains dry with pressure head values lower than −20.4 m.

Pressure head time series were affected by some gaps, from few days to weeks, during which values exceeded downward the functioning limit of tensiometers and Watermark sensors. Moreover, the functioning of few sensors was interrupted for a limited period of time due to damages caused to the equipment by the grazing of wild boars. In these

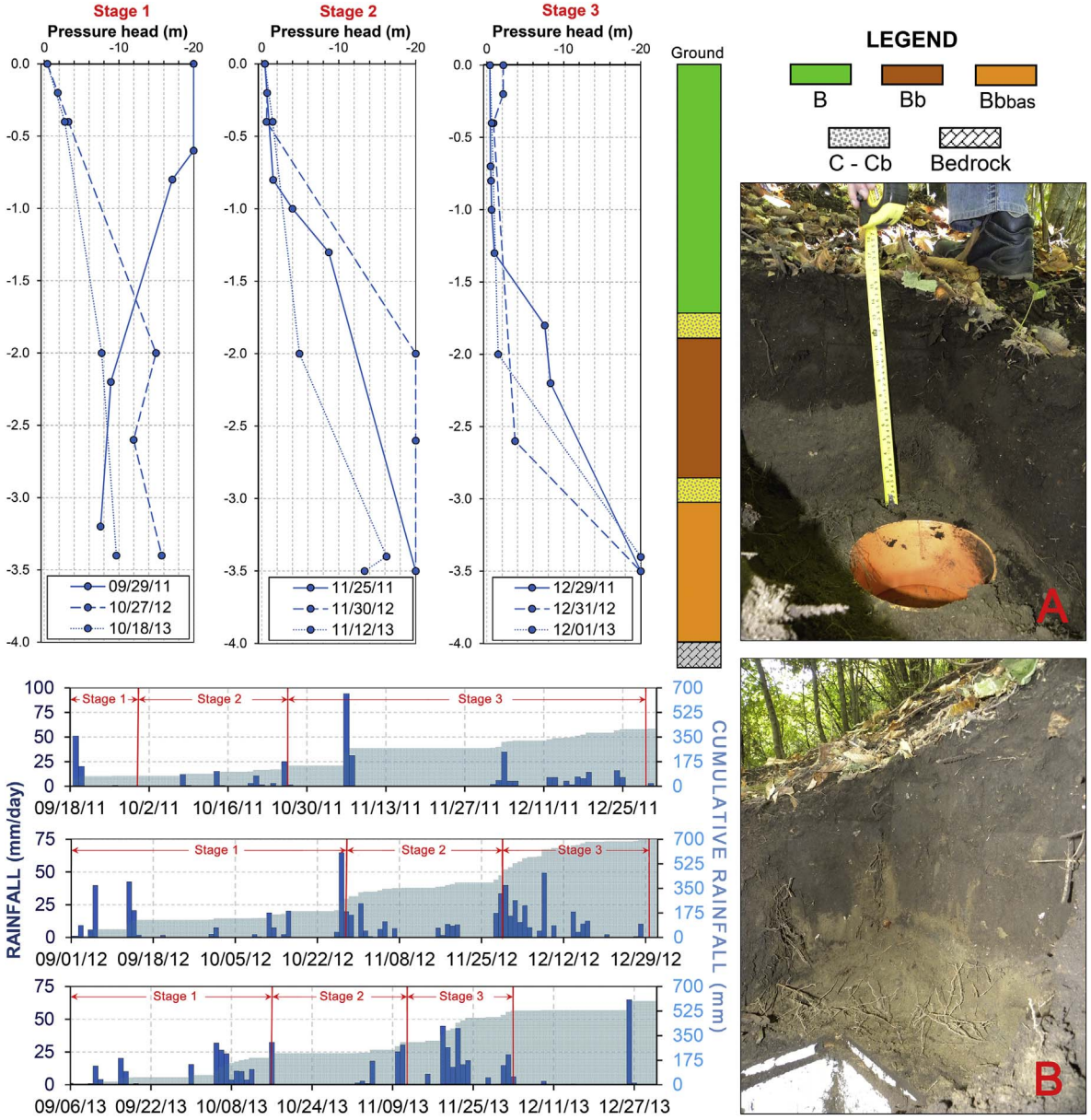

Fig. 6. Vertical profiles of pressure head measured at hydrological stages 1, 2 and 3 for years 2011, 2012 and 2013. Pictures of the infiltration front deepening into test pits at the beginning of the rainy period are also shown in boxes on the right (A and B).

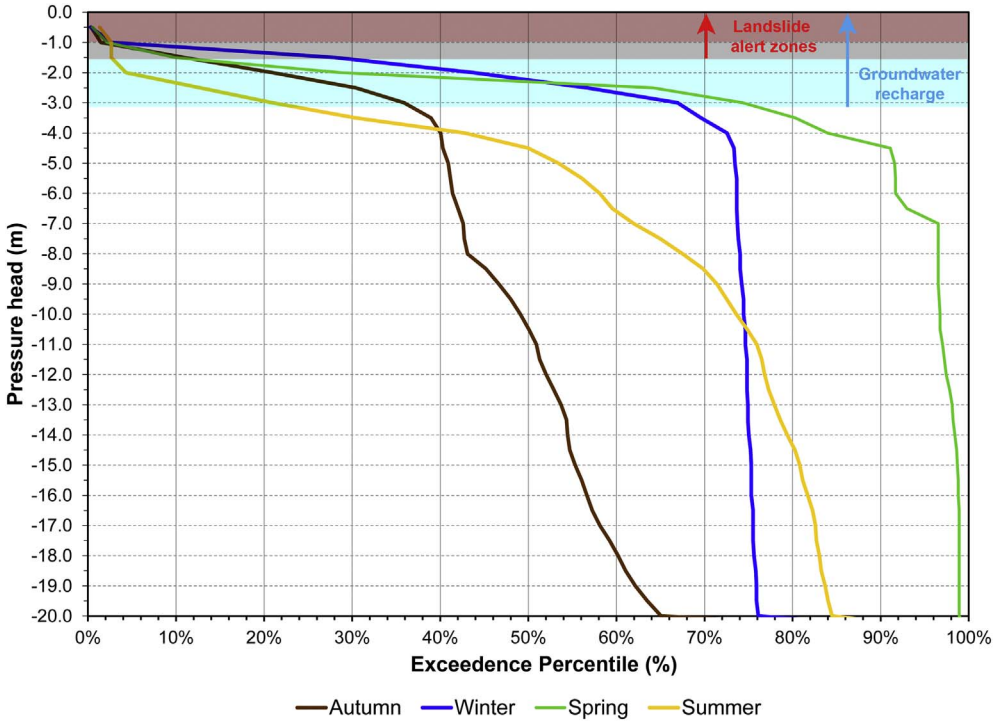

Fig. 7. Seasonal Duration Curves of mean pressure head recorded in the whole ash-fall pyroclastic mantle for the monitoring period. Shaded areas indicate landslide alert ($h > -1.5$ m and $h > -1.0$ m) and groundwater recharge ($h > -3.06$ m) zones. Seasonal time intervals: 23 Sept.–22 Dec. (Autumn); 23 Dec.–20 Mar. (Winter); 21 Mar.–21 Jun. (Spring); 22 Jun.–22 Sept. (Summer).

cases, recording were resolved by an interpolation of recorded data across the short non-functioning periods.

4.1. Frequency analysis of pressure head time series

To comprehend the hydrological behavior of the ash-fall pyroclastic soil cover, pressure head time series were analyzed by the calculation of seasonal Duration Curves (DCs), which allowed estimating exceedence frequencies for given values of pressure head. DCs were reconstructed for subsets identified by the subdivision of the whole time series (December 2010–December 2014), according to seasonal periods and taking into account both the mean value of the whole pyroclastic mantle and each soil horizon.

The first analysis was carried out for the mean value of the whole ash-fall pyroclastic soil mantle and considering the seasonal variability of pressure head values (Fig. 7). In this analysis, the whole pyroclastic mantle revealed the existence of a variable distribution of pressure head values during seasons, which can be subdivided approximately in three main frequency classes. The first is represented by values comprised from -0.5 m to about -4.0 m, which passes to the second one through a marked knee point in the DCs, down to the lower functioning limit of Watermark sensors ($h < -20.4$ m), and the third by values not recorded because exceeding the abovementioned limit. The first class has different exceedence percentiles during seasons reaching about 40% in autumn, 74% in winter, 84% in spring and 40% in summer. The second class has frequencies comprised between the preceding values and the respective exceedence percentiles of 64% for autumn (24%), 76% for winter (2%), 99% for spring (15%) and 65% for summer (25%), whose complementary values indicate also the frequencies of pressure head not measured because exceeding the functioning limit of the Watermark sensors.

The subsequent analysis was carried out by the reconstruction of seasonal DCs obtained for each soil horizon (Fig. 8). During autumn, a composite hydrological state characterizes the ash-fall pyroclastic soil mantle with the B horizon in a condition wetter than the deeper Bb horizon as it is clearly showed respectively by the exceedence percentiles of 60% and 12%, for the pressure head value of -3.0 m that marks evident knee points on the respective DCs. The Bb_{basal} horizons shows a much drier condition, if compared to the shallower soil horizons, with pressure head comprised between -6.0 m and the lower functioning limit of the Watermark sensors ($h < -20.4$ m). For the three soil horizons, pressure head values reached the lower limit of functioning of Watermark sensors ($h < -20.4$ m), with frequencies given by the complementary values of the exceedence percentiles of 88% for B horizon (12%), 36% for Bb horizon (64%) and 46% for Bb_{basal} horizon (54%).

The winter season is characterized by strong and variable wetting conditions of the B and Bb horizons which reach respectively exceedence percentiles of 96% and 46% for the pressure head value of -3.0 m and marked knee points on the respective DCs. Contrastingly, the Bb_{basal} horizon progresses in drying as it is showed by pressure head values limited in the range lower than -14.0 m. During this season, pressure head values exceed the lower functioning limit of Watermark sensors only for the Bb horizon, with a frequency of 26%, and for the Bb_{basal} horizon, with a frequency of 98%. In the spring season, the whole ash-fall pyroclastic soil cover reaches the most homogeneous hydrological condition with a general strong advance of wetting for the Bb and Bb_{basal} horizons and a slight drying for the B horizon, due to the downward advance of the infiltration front and soil moisture redistribution processes. The wettest condition is clearly showed by knee points on the DCs, ranging from -3.0 m and -4.0 m, with exceedence percentiles ranging from 88% to 98%. Moreover, the wetter condition of this period is demonstrated by the lack of pressure head values exceeding the lower functioning limit of Watermark sensors for the B and Bb horizon and with a frequency of 12% for the Bb_{basal} horizon. During summer, in comparison with the spring season, the ash-fall pyroclastic soil cover shows a drying process of soil horizons decreasing with the depth as it clearly appears by exceedence percentiles of 52%, 44% and 86% of the B, Bb and Bb_{basal} horizons respectively for pressure head value of -5.0 m. The B and Bb horizons show a more homogeneous drying due to the lack of precise knee points on the DCs. Moreover, the DC of the B horizon shows an exceedence percentile of 5% for pressure head values greater than -2.0 m due the effect of sporadic summer rainstorms. For the Bb_{basal} horizon, a variable drying is testified by a marked knee point corresponding approximately to a pressure head value of -4.5 m.

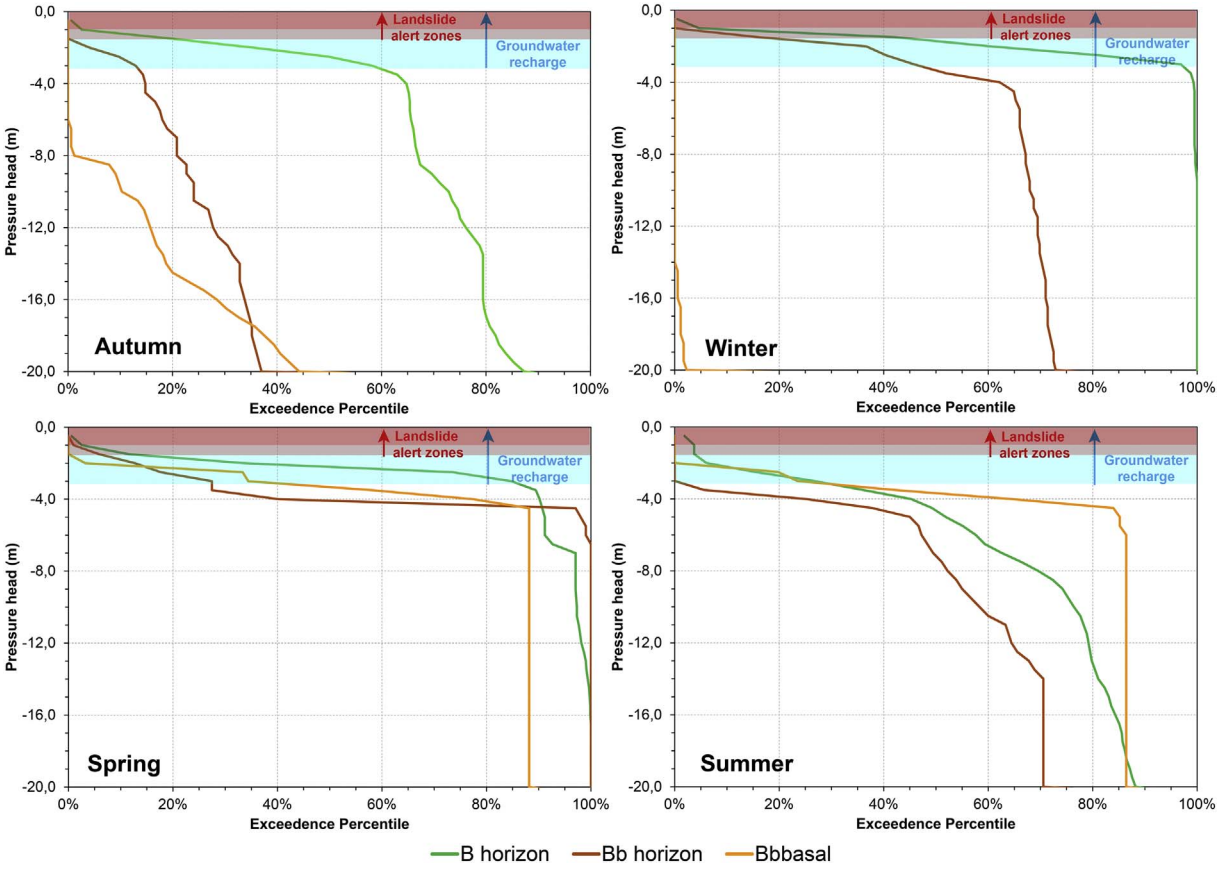

Fig. 8. Seasonal Duration Curves for pressure head values recorded for B, Bb and Bb_{basal} soil horizons. Shaded areas indicate landslide alert ($h > -1.5$ m and $h > -1.0$ m) and groundwater recharge ($h > -3.06$ m) zones. Seasonal time intervals: 23 Sept.–22 Dec. (Autumn); 23 Dec.–20 Mar. (Winter); 21 Mar.–21 Jun. (Spring); 22 Jun.–22 Sept. (Summer).

Pressure head values, measured in the period from December 2010 to December 2014, were transformed in the correspondent volumetric water content values by the SWRCs (Table 3), allowing calculating SWD time series by the Eq. (3). According to rainfall seasonal patterns, the SWD time series present relevant fluctuations with maxima occurring from February to April, while minima from September to October (Fig. 9 and Table 6). The highest value of SWD was observed in March 2011 with 1320 mm and the lowest value in October 2011 with 935 mm. For this hydrological year, the estimated net loss of soil water retained by the ash-fall pyroclastic soil cover, due to both evapotranspiration and drainage toward the bedrock, was of 385 mm. The same assessment was carried out for the other hydrological years allowing the estimation of annual ranges of SWD (Table 6). The SWD seasonal fluctuations were also compared with the SWD levels corresponding to SAT, FC and PWP, estimated equal to 2084 mm, 1121 mm and 507 mm respectively (Fig. 9). Across the monitored years, the SWD was recognized fluctuating around the FC level, thus allowing the identification of periods of the rainy season with water content

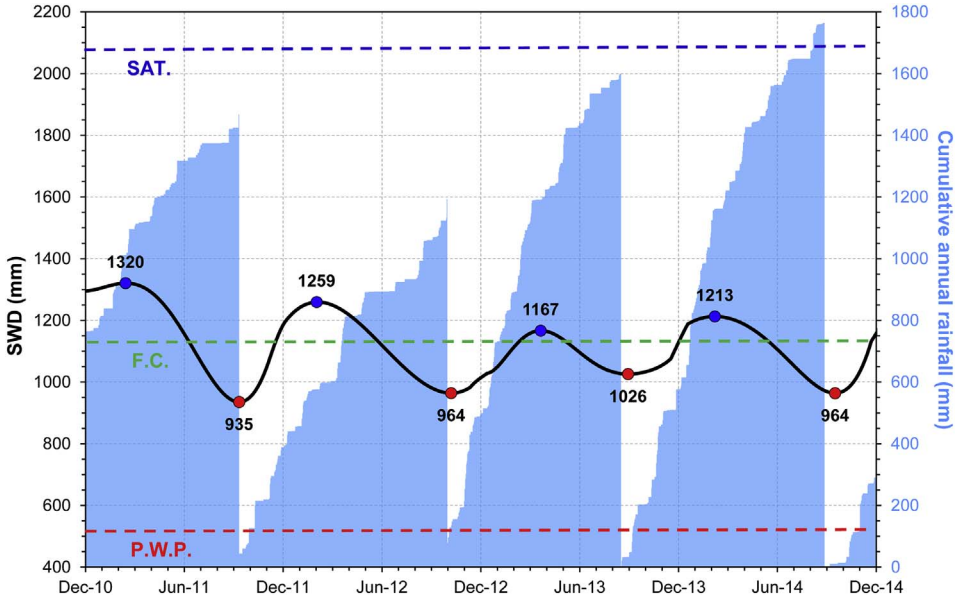

Fig. 9. Estimated time series of Soil Water Depth (SWD) for the monitoring site in comparison with the annual rainfall cumulative curves. SWD for Saturation (SAT), Field Capacity (FC) and Permanent Wilting Point (PWP) pressure head levels are also shown (dashed horizontal lines). Yearly maximum (red dots) and minimum values (blue dots) are shown. (For interpretation of the references to colour in this figure legend, the reader is referred to the web version of this article.)

Table 6
Cumulative rainfall and descriptive statistics of SWD estimated for the four hydrological monitoring years.

Hydrological year		Cumulated rainfall (mm)	SWD (mm)			
Beginning	End		Min	Mean	Max	Range
01/10/2010	07/10/2011	1468	935	1156	1320	385
07/10/2011	27/10/2012	1192	964	1109	1259	295
27/10/2012	14/09/2013	1599	1026	1087	1167	141
14/09/2013	26/09/2014	1764	964	1106	1212	248
					Mean	267

exceeding the FC one. In these periods, soil water available for unsaturated gravity drainage, forming both unsaturated throughflow within slopes and percolation recharging the underlying karst aquifer, were recognized occurring with a variability depending on annual amount and temporal patterns of rainfall.

Based on results of preceding studies (Allocca et al., 2015; De Vita et al., 2013; Napolitano et al., 2016) three levels of pressure head were identified as significant for hydrological processes related to landslide initiation and groundwater recharge. About the first issue, the effect of a rainfall event has a different impact on the slope stability depending on the antecedent soil hydrological status as it has been demonstrated by the effect of antecedent hydrological conditions on Intensity-Duration rainfall thresholds (Napolitano et al., 2016). In such a view, the temporal probability of rainfall induced landslides is not simply related to the probability of a given rainfall event but to the compound probability of the latter with that of assumed antecedent hydrological conditions (Glade et al., 2000). At this scope, the exceedence percentiles of pressure head values of − 1.00 m and − 1.50 m were considered well representing temporal probabilities of antecedent hydrological conditions potentially critical for slope stability, when in combination with high-intensity and duration rainfall events. It is demonstrated by the recurrence of landslides during winter and early spring, when these values of pressure head typically occur in the ash-fall pyroclastic soil mantle. In particular, pressure head levels of − 1.00 m and − 1.50 m were conceived as landslide alert zones with an increasing level of proneness to landslide triggering under a heavy rainfall events. For pressure head values lower than − 1.50 m, a hydrological condition of the ash-fall pyroclastic soil cover less predisposed to slope instability was identified as a no alert zone. Moreover, the pressure head value corresponding to FC (h > − 3.06 m) was considered significant for identifying groundwater recharge because representing a threshold value above which gravity drainage toward the saturation zone can occur. Therefore, the exceedence percentile of this value identifies the temporal frequency of groundwater recharge process occurring for

Table 7
Seasonal exceedence percentiles (%) of pressure head measured for the whole ash-fall pyroclastic soil mantle.

Processes	Groundwater recharge	Gravity drainage		
	Landslide	Alert zones		No alert zone
Pressure head (h)		> − 1.00 m	> − 1.50 m	> − 3.06 m
Whole ash-fall pyroclastic cover				
Autumn		1.5	11.0	35.9
Winter		2.7	28.1	66.9
Spring		2.2	9.9	74.4
Summer		2.7	2.7	21.0
Whole period		2.3	13.3	51.1

Table 8
Seasonal exceedence percentiles (%) of pressure head measured for soil horizons of the ash-fall pyroclastic soil mantle.

Processes	Groundwater recharge	Gravity drainage		
	Landslide	Alert zones		No alert zone
Pressure head		> − 1.00 m	> − 1.50 m	> − 3.06 m
B horizon				
Autumn		2.6	19.7	58.2
Winter		4.7	42.2	96.9
Spring		2.6	11.5	84.8
Summer		3.7	3.7	26.7
Whole period		3.4	18.1	67.7
Bb horizon				
Autumn		0	0	13.0
Winter		0	16.0	45.8
Spring		1.0	5.9	27.5
Summer		0	0	0
Whole period		0.1	6.3	23.2
Bb_{basal} horizon				
Autumn		0.	0	0
Winter		0	0	0
Spring		0	0	34.4
Summer		0	0	23.5
Whole period		0	0	9.9

greater values of pressure head. Seasonal exceedence percentiles corresponding to the abovementioned three levels were evaluated for both the whole ash-fall pyroclastic soil cover (Table 7) and considering principal soil horizons (Table 8).

By the analysis of seasonal exceedence percentile values calculated for the whole ash-fall pyroclastic mantle (Table 7 and Fig. 7), pressure head values in winter were observed greater than − 1.00 m, with a frequency of 2.7%, and greater than − 1.50 m, with a frequency of 28.1%. Instead, pressure head values were greater than − 3.06 m, indicating the occurrence of groundwater recharge process, with frequencies variable from 74.4% in winter to 21% in summer.

Seasonal exceedence percentiles estimated for B, Bb and Bb_{basal} horizons indicated a complex hydrological response dynamics controlling predisposition to landslide triggering and timing of groundwater recharge process (Table 8 and Fig. 8). For the B horizon, maximum frequencies of pressure head values greater than − 1.00 m and − 1.50 m were estimated respectively equal to 4.7% and 42.2% during winter. Instead, frequency of pressure head value greater than − 3.06 m was estimated varying from 96.6% in winter and 26.7% during summer.

For the Bb horizon the highest frequencies of pressure head were estimated equal to 1.0% in spring, for values greater than − 1.00 m, and equal to 16.0% in winter, for values greater than − 1.50 m. Frequency of pressure head value greater than − 3.06 m was estimated varying from 45.8% in winter and 0.0% during summer.

For the Bb_{basal} horizon the frequencies of pressure head value greater than − 1.00 m and − 1.50 m were always null for all seasons. Instead, frequency of pressure head value greater than − 3.06 m was estimated varying from 34.4% in spring and 0.0% during autumn and winter.

4.2. Distributed hydro-geomorphological modelling of the ash-fall pyroclastic soil coverings

Given the dependence of the SWD on the thickness of ash-fall pyroclastic soil coverings a hydro-geomorphological model was elaborated by coupling results showed in the preceding paragraph with the distribution model of ash-fall pyroclastic soils along slopes (De Vita et al., 2006a; De Vita and Nappi, 2013). For instance, by the Eq. (3) the

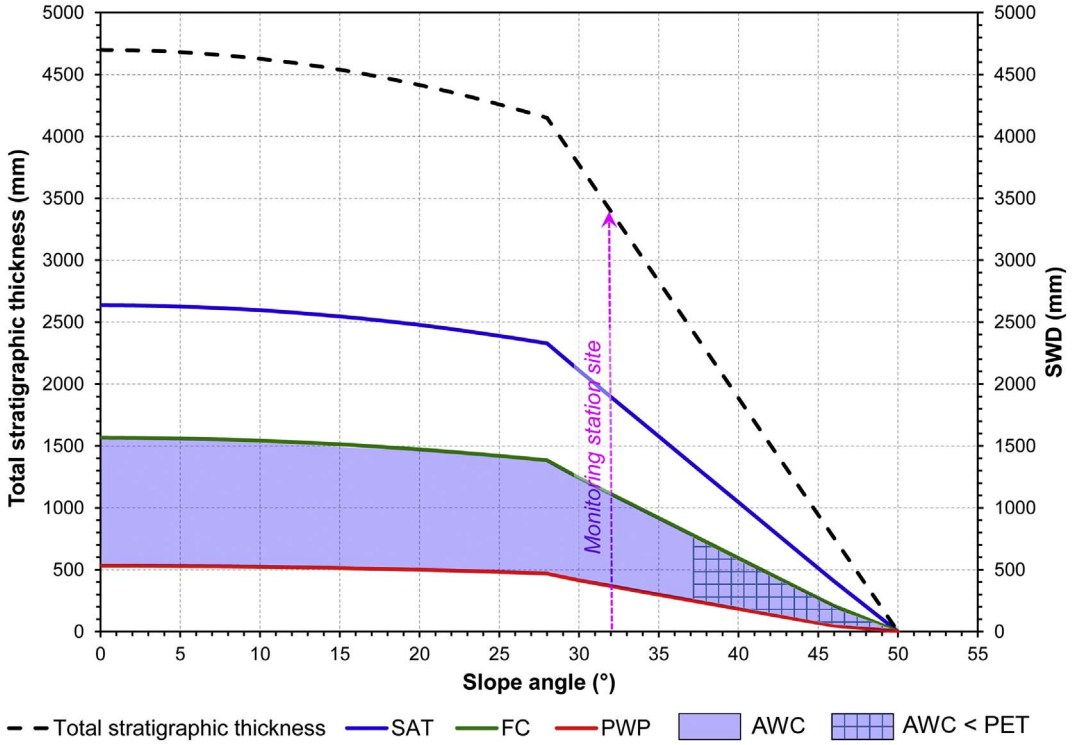

Fig. 10. Hydro-geomorphological model related to the total theoretical ash-fall pyroclastic soil thickness fallen in the monitoring station site (z0 = 4.7 m). Total stratigraphic thickness in different slope angle conditions and Soil Water Depth (SWD) stored in the ash-fall pyroclastic soil cover, for pressure head levels of saturation (SAT), field capacity (FC) and permanent wilting point (PWP), are shown. The Soil Water Depth (SWD) corresponding to the Available Water Content (AWC) is the shaded violet area. The morphological site conditions are indicated by the vertical line passing through the slope angle value of 32°. (For interpretation of the references to colour in this figure legend, the reader is referred to the web version of this article.)

decrease of ash-fall pyroclastic soil thickness, as the slope angle increases, determines a progressive reduction of Soil Water Depth (SWD) corresponding to SAT, FC and PWP levels down to their annulment for values of slope angle > 50°. Accordingly, also the Soil Water Depth (SWD) corresponding to the Available Water Content (AWC) reduces as the slope angle increases, down to its annulment for slope angle values > 50°. In such a way, the SWD values for SAT, FC and PWP were estimated considering the total theoretical ash-fall pyroclastic soil thickness fallen in the monitoring station site (z_0 = 4.7 m) and the control of the slope angle (Fig. 10).

The annual PET was estimated ranging from 507 mm to 577 mm and with an average value of 547 mm (Table 9). By comparing this range of annual PET with the SWD corresponding to AWC, it is possible understanding that the PET demand is generally lower except for thickness of the ash-fall pyroclastic soil mantle lower than 2.0 m, existing for slope angle values > 37° (Fig. 10). For instance, for slope angle values higher than 37°, ash-fall pyroclastic soil cover become thinner than 2.0 m and the PET demand is limited by the AWC retained by the ash-fall soil covering. Therefore, AET is equal to the PET in the slope angle range lower than 37°, instead it is limited to the AWC for greater slope angle values. Namely the evapotranspiration process can be considered energy-limited and water-limited (Budyko, 1974), respectively in the two slope angle ranges.

The results obtained for the monitoring site can be exported at the distributed scale considering different values of z_0 (Fig. 1) and slope angle control.

Table 9
Annual Potential Evapotranspiration (PET) estimated by the Thorntwaithe equation and representative of the monitoring station area.

PET (mm)	1999	2000	2001	2002	2003	2004	2005	2006
	550	552	544	541	565	535	507	536
	2007	2008	2009	2010	2011	2012	2013	2014
	551	549	554	526	555	577	555	556

5. Discussion

Analyses presented in this research were focused chiefly to understand and model hydrological behavior of the ash-fall pyroclastic soil coverings at the seasonal time scale. Results obtained are not fully comparable with those of other researches based similarly on field hydrological monitoring of infiltration process at a shorter time scale (Montgomery et al., 1997; Torres et al., 1998; Ebel and Loague, 2008), which analyzed the magnitude and velocity of the rapid hydrologic response propagating through the unsaturated zone and effects of both antecedent hydrological status and the shape of the SWRCs. Moreover, no other cases of DC analysis of soil pressure head time series are known in literature.

In the four-years monitoring period, during rainy periods, typically occurring from November to March, pressure head records showed the highest values, well matching with those previously measured in other experimental monitoring sites in ash-fall pyroclastic soil mantled slopes (Cascini et al., 2014; Damiano et al., 2012; Greco et al., 2013; Comegna et al., 2013; Pagano et al., 2010; Papa et al., 2013b). Remarkably, during rainy periods saturation conditions were not observed although near-saturation conditions were transitorily reached in the shallower B horizon only. Starting from the late spring until the early autumn, in the period from April to October, an abrupt decrease of pressure head was measured. These measured values, especially in August and September, showed a difference with the lowest values measured by the above-mentioned authors through tensiometers only, which were limited to pressure head value of about − 8.0 m. In fact, principally due to evapotranspiration process and a gradual decrease of rainfall events, pressure head values reached and exceeded the measurement limit of Watermark sensors (h < − 20.4 m) in the whole pyroclastic mantle. The decrease of pore pressure did not occur simultaneously at all

depths, but earlier in the upper part of the cover (B horizon) and gradually in the deeper horizons (Bb and Bb_{basal}). Moreover, during the rainy period, pressure head values increased in the upper soil horizons while they continued reducing in the deeper ones. Such a hydrological behavior was reversed during the summer period, with deeper soil horizons wetter than the surficial ones. These opposing dynamics can be associated to a re-equilibrium of pore pressure within the deeper horizons due to the effect of deeper roots of chestnut trees and secondly due to the existence of a vertical and/or lateral unsaturated water flow within the cover. The very low pressure head values recorded in the dry period do not appear a singularity as it results by other field hydrological monitoring experiences, carried out in a saprolitic hillslope through heat dissipation matric water potential sensors (Leung and Wang Wai Ng, 2013), which allowed measuring values down to about − 19.0 m. These results confirm a hydrological dynamics of soil coverings potentially wider than the typical measurement range of tensiometers and therefore the limited applicability of the latters for a comprehensive soil hydrological monitoring.

From DCs analysis it was possible to comprehend that critical conditions for slope stability can occur principally during winter and spring when > 50% of pressure head values ranged between − 0.3 m and − 2.0 m. In these cases heavy rainfall events causing infiltration within ash-fall pyroclastic soil covering and increase of unsaturated hydraulic conductivity in the upper horizon can promote unsaturated throughflow and the downslope formation of saturation wedges at hydrogeological discontinuities corresponding to a decrease of hydraulic transmissivity (De Vita et al., 2006b; Reid et al., 1988), specifically represented by the three principal geomorphological conditions (De Vita et al., 2013): pinch out of C horizons in convex slopes with knick points marking a rapid increase of slope angle > 35°; road cuts; pinch out of the whole ash-fall pyroclastic soil mantle above vertical rocky scarps. On the contrary, higher slope stability condition exists during summer period, even during heavy rainstorms. Particular conditions occur in autumn and winter, when the cover is characterized by high pressure head values in the shallower zone and lower values in deeper ones. These conditions can be considered intermediate in term of probability of debris flow triggering.

The hydro-geomorphological modelling of soil coverings, based on an empirical relationship between soil thickness and slope angle, can be considered as a novel approach for the distributed analysis of hydrological regime of ash-fall pyroclastic mantle, which can be conceived similar to methods used by other authors (e.g. Iida, 1999). Among principal results of this approach is the recognition that for the higher slope angle range, characterized by a critical condition for slope stability, the lower Soil Water Depth corresponding to AWC (Fig. 10) permits during the rainy season a more enhanced and rapid fluctuation of pressure head from the PWP to and above the FC, thus determining a more favorable condition for the formation of unsaturated throughflow.

Hydrological monitoring of ash-fall pyroclastic soil cover and analysis of pressure head DCs allowed also understanding the timing of groundwater recharge showing that hydrological conditions for gravity drainage (h > − 3.06 m) can occur with an exceedence percentile of 51.1%, if considering the whole ash-fall pyroclastic soil cover and the whole monitoring period (Table 7). By analyzing the seasonal hydrological behavior of single soil horizons, conditions for the gravity drainage were found varying during the year and with depth. For the shallower B horizon, gravity drainage exists during all seasons with variable exceedence percentiles. Instead, for the Bb and the Bb_{basal} horizon, these conditions do not exist for all seasons (Table 8 and Fig. 8). In particular, according to the delayed hydrological response, field measurements showed that gravity drainage can occur in the Bb_{basal} horizon only during spring and summer. Considering that the Bb_{basal} horizon is at the interface with the carbonate bedrock (Table 1), it can be argued that timing of the gravity drainage of this horizon controls the groundwater recharge of the underlying carbonate aquifer, unless the occurrence of preferential flow phenomena (Mirus and Nimmo, 2013).

The proposed hydro-geomorphological model can be considered significant also for the assessment of groundwater recharge process at a distributed scale because it takes into account the effect of thickness of ash-fall pyroclastic soil mantle on soil water storage, which controls quantity and timing of groundwater recharge (Appels et al., 2015). Specifically, outcomes of this research could be applied to model the groundwater recharge taking also into account effects of morphological conditions that control both ash-fall pyroclastic soil thickness along slopes and AWC available for evapotranspiration process. Finally, it is important to point out that monitoring results showed the involvement in the hydrological response dynamics, due to infiltration, water redistribution and evapotranspiration processes, of the whole ash-fall pyroclastic soil cover, characterized by a vertical thickness of about 4.0 m in the monitoring site. Such behavior can be related to the depth of chestnut root apparatuses, thus extendable to the most part of the peri-Vesuvian mountain ranges, characterized by the same land cover.

6. Conclusions

Studies in the last decades showed as the hydrological monitoring of soil coverings can allow the comprehension of hydrological dynamics leading to both shallow slope instabilities and groundwater recharge. Researches about these two topics have in general considered the hydrological behavior of regolith deposits, both of residual and transported types, coupled with the uppermost pedogenetic horizons (top soil), but rarely of allocthonous deposits such as ash-fall pyroclastic soils. Therefore, understanding hydrological behavior and regime of ash-fall pyroclastic deposits is a relevant and novel scientific theme crossing through geology, geomorphology, and hydrology whose applications can be considered relevant to different scopes of environmental management and territorial planning. Also in the case of ash-fall pyroclastic deposits mantling peri-Vesuvian hillslopes, field hydrological monitoring is very important for assessing hazard to debris flow triggering and groundwater recharge of underlying karst aquifers.

Obtained results allow recognizing the ash-fall pyroclastic soil mantle as a complex geo-hydrological system in which antecedent conditions due to seasonality play an important role in controlling slope stability during rainfall events. Among principal and novel results achieved in this study is the frequency analysis of pressure head within the ash-fall pyroclastic soil mantle by the reconstruction of seasonal DCs. By this analysis the temporal frequencies of certain pressure head levels are known, permitting, for the first time, to assess temporal probability of antecedent hydrological conditions that predispose to landslide triggering as well as amount and temporal patterns of the recharge of underlying karst aquifers.

Therefore, the proposed approach, based on field hydrological monitoring of ash-fall pyroclastic coverings is fundamental to give a more comprehensive probabilistic character to rainfall thresholds and related early warning systems. At the same time, results obtained by this approach are also useful to comprehend the spatially variable dynamics of groundwater recharge depending on evapotranspiration process and thickness of ash-fall pyroclastic soil mantle.

Further studies, starting from such basis will be oriented to a more consistent probabilistic analysis of hazard to debris flow triggering under different antecedent hydrological conditions and rainfall patterns. Finally, the proposed study can be considered potentially advancing knowledge on landslide and groundwater recharge issues of other peri-volcanic mountainous areas of the world, which are similarly covered by ash-fall pyroclastic soils.

Acknowledgments

The research was funded by: a) Governmental Commissariat for the Hydrological Emergency in the Campania Region (Act No. 1902 of 25 September 2001); b) PRIN Project (2010 − 2011) “*Time-Space prediction*

of high impact landslides under changing precipitation regimes," funded by the Ministry for Education, University and Research (MIUR-Italy); c) Ph.D. Program (2014–2016) of Dipartimento di Scienze della Terra, dell'Ambiente e delle Risorse, University of Naples Federico II.

References

Allocca, V., De Vita, P., Manna, F., Nimmo, J.R., 2015. Groundwater recharge assessment at local and episodic scale in a soil mantled perched karst aquifer in southern Italy. J. Hydrol. 529, 843–854.

Allocca, V., Manna, F., De Vita, P., 2014. Estimating annual groundwater recharge coefficient for karst aquifers of the southern Apennines (Italy). Hydrol. Earth Syst. Sci. 18, 803–817.

Appels, W.M., Graham, C.B., Freer, J.E., McDonnell, J.J., 2015. Factors affecting the spatial pattern of bedrock groundwater recharge at the hillslope scale. Hydrol. Process. 29, 4594–4610.

Bordoni, M., Meisina, C., Valentino, R., Lu, N., Bittelli, M., Chersich, S., 2015. Hydrological factors affecting rainfall-induced shallow landslides: From the field monitoring to a simplified slope stability analysis. Eng. Geol. 193, 19–37.

Budyko, M.I., 1974. Climate and Life. Academic Press, New York (508 pp).

Caine, N., 1980. The rainfall intensity-duration control of shallow landslides and debris flows. Geogr. Ann. 62A (1–2), 23–27.

Calcaterra, D., Parise, M., Palma, B., Pelella, L., 2000. The influence of meteoric events in triggering shallow landslides in pyroclastic deposits of Campania, Italy. In: Bromhead, E., Dixon, N., Ibsen, M.L. (Eds.), Landslides in research, theory and practice, Proc. 8th Int. Symposium on Landslides, Cardiff, UK, pp. 209–214.

Cascini, L., Cuomo, S., Guida, D., 2008. Typical source areas of May 1998 flow-like mass movements in the Campania region Southern Italy. Eng. Geol. 96, 107–125.

Cascini, L., Sorbino, G., Cuomo, S., Ferlisi, S., 2014. Seasonal effects of rainfall on the shallow pyroclastic deposits of the Campania region (southern Italy). Landslides 11, 779–792.

Catani, F., Segoni, S., Falorni, G., 2010. An empirical geomorphology-based approach to the spatial prediction of soil thickness at catchment scale. Water Resour. Res. 46, 1–15.

Celico, P., Guadagno, F.M., Vallario, A., 1986. Proposta di un modello interpretativo per lo studio delle frane nei terreni piroclastici. Geol. Appl. Idrogeol. 21, 173–193.

Cole, P.D., Scarpati, C., 2010. The 1944 eruption of Vesuvius, Italy: combining contemporary accounts and field studies for a new volcanological reconstruction. Geol. Mag. 147 (3), 391–415.

Comegna, L., Damiano, E., Greco, R., Guida, A., Olivares, L., Picarelli, L., 2013. Effects of the vegetation on the hydrological behavior of a loose pyroclastic deposit. Procedia Environ Sci 19, 922–931.

Crosta, G.B., Dal Negro, P., 2003. Observations and modelling of soil slip-debris flow initiation processes in pyroclastic deposits: the Sarno 1998 event. Nat. Hazards Earth Syst. Sci. 3, 53–69.

Cruden, D.M., Varnes, D.J., Turner, A.K., Schuster, R.L., 1996. Landslide types and processes. In: Landslides, investigation and mitigation. Transportation Research Board. US National Research Council, Special Report, Washington DC. 247. pp. 36–75.

D'Argenio, B., Pescatore, T., Scandone, P., 1973. Schema geologico dell'Appennino Meridionale (Campania e Lucania). Proceedings of the meeting "Moderne vedute sulla geologia dell'Appennino". Quaderni Accademia Nazionale dei Lincei. 183. pp. 49–72.

Dalrymple, T., 1960. Flood-Frequency Analyses. Geological Survey. Water-Supply Paper. 1543-A.

Damiano, E., Olivares, L., Picarelli, L., 2012. Steep-slope monitoring in unsaturated pyroclastic soils. Eng. Geol. 137–138, 1–12.

de Riso, R., Budetta, P., Calcaterra, D., Santo, A., 1999. Le colate rapide in terreni piroclastici del territorio campano. In: Peila, D. (Ed.), Proceedings of "Convegno su previsione di movimenti franosi", Trento, 17–18-19 June 1999, GEAM, pp. 133–150.

DeRose, R.C., Trustrum, N.A., Blaschke, P.M., 1991. Geomorphic change implied by regolith-slope relationship on steepland hillslope, Taranaki, New Zealand. Catena 18, 489–514.

De Vita, P., Agrello, D., Ambrosino, F., 2006a. Landslide susceptibility assessment in ash-fall pyroclastic deposits surrounding Mount Somma-Vesuvius. Application of geophysical surveys for soil thickness mapping. J. Appl. Geophys. 59, 126–139.

De Vita, P., Celico, P., Siniscalchi, M., Panza, R., 2006b. Distribution, hydrogeological features and landslide hazard of pyroclastic soils on carbonate slopes in the area surrounding Mount Somma-Vesuvius. Ital. J. Eng. Geol. Environ. 1, 1–24.

De Vita, P., Di Maio, R., Piegari, E., 2012. A study of the correlation between electrical resistivity and matric suction for unsaturated ash-fall pyroclastic soils in the Campania region (southern Italy). Environ. Earth Sci. 67, 787–798.

De Vita, P., Napolitano, E., Godt, J., Baum, R., 2013. Deterministic estimation of hydrological thresholds for shallow landslide initiation and slope stability models: case study from the Somma-Vesuvius area of southern Italy. Landslides 10, 713–728.

De Vita, P., Nappi, M., 2013. Regional distribution of ash-fall pyroclastic soils for landslide susceptibility assessment. In: Margottini (Ed.), Lanslide Science and Practice. 3. Springer-Verlang Heidelberg, pp. 103–109.

De Vita, P., Piscopo, P., 2002. Influences of hydrological and hydrogeological conditions on debris flows in peri-Vesuvian hillslopes. Nat. Hazards Earth Syst. Sci. 2, 1–9.

Ebel, B.A., Loague, K., 2008. Rapid simulated hydrologic response within the variably saturated near surface. Hydrol. Process. 22, 464–471.

Fusco, F., De Vita, P., 2015. Hydrological behavior of ash-fall pyroclastic soil mantled slopes of the Sarno Mountains (Campania – southern Italy). Rend. Online Soc. Geol. Ital. 35, 148–151.

Fusco, F., De Vita, P., Napolitano, E., Allocca, V., Manna, F., 2013. Monitoring the soil suction regime of landslide-prone ash-fall pyroclastic deposits covering slopes in the Sarno area (Campania – southern Italy). Rend. Online Soc. Geol. Ital. 24, 146–148.

Glade, T., Crozier, M., Smith, P., 2000. Applying probability determination to refine landslide-triggering rainfall thresholds using an empirical "antecedent daily rainfall model". Pure Appl. Geophys. 157, 1059–1079.

Greco, R., Comegna, L., Damiano, E., Guida, A., Olivares, L., Picarelli, L., 2013. Hydrological modelling of a slope covered with shallow pyroclastic deposits from field monitoring data. Hydrol. Earth Syst. Sci. 17, 4001–4013.

Healy, R.W., 2010. Estimating Groundwater Recharge. Cambridge University Press (256 pp. ISBN. 978-0521863964).

Helsel, D.R., Hirsch, R.M., 2002. Statistical Methods in Water Resources. Techniques of Water-Resources Investigations of the United States Geological Surveypp. 4 (510pp).

Hungr, O., Leroueil, S., Picarelli, L., 2014. The Varnes classification of landslide types, an updated. Landslides 11, 167–194.

Iida, T., 1999. A stochastic hydro-geomorphological model for shallow landsliding due to rainstorm. Catena 34, 293–313.

Jakob, M., Hungr, O., 2005. Debris-flow Hazards and Related Phenomena. Springer-Verlang (739 pp. ISBN 978-3-540-27129-1).

Kirkby, M.J., 1978. Hillslope Hydrology. John Wiley and Sons (389 pp. ISBN 978-0-471-99510-4).

Kirkham, M.B., 2005. Principles of Plant and Soil Water Relations. Elsevier (500 pp. ISBN 978-0-12-420022-7).

Kutilek, M., Nielsen, D.R., 1994. Soil Hydrology. Catena-Verlang (370 pp.).

Leung, A.K., Wang Wai Ng, C., 2013. Seasonal movement and groundwater flow mechanism in an unsaturated saprolitic hillslope. Landslides 10, 455–467.

Lirer, L., Pescatore, T., Booth, B., Walker, J.P.L., 1973. Two Plinian pumice-fall deposits from Somma-Vesuvius. Geol. Soc. Am. Bull. 84, 759–772.

Lu, N., Godt, J.W., 2013. Hillslope Hydrology and Stability. Cambrige University Press (458 pp. ISBN 978-1107021068).

Lu, N., Likos, W.J., 2004. Unsaturated Soil Mechanics. Wiley (556 pp. ISBN 978-0-471-44731-3).

Mancarella, D., Doglioni, A., Simeone, V., 2012. On capillary barrier effects and debris slide triggering in unsaturated layered covers. Eng. Geol. 147–148, 14–27.

Mirus, B.B., Nimmo, J.R., 2013. Balancing practicality and hydrologic realism: a parsimonious approach for simulating rapid groundwater recharge via unsaturated-zone preferential flow. Water Resour. Res. 49, 1458–1465.

Montgomery, D.R., Dietrich, W.E., Torres, R., Anderson, S.P., Heffner, J.T., Loague, K., 1997. Hydrologic response of a steep, unchanneled valley to natural and applied rainfall. Water Resour. Res. 33, 91–109.

Mostardini, F., Merlini, S., 1986. Appennino centro meridionale. Sezioni geologiche e proposta di modello strutturale. Memorie Società Geologica Italiana. 35. pp. 177–202.

Napolitano, E., Fusco, F., Baum, R.L., Godt, J.W., De Vita, P., 2016. Effect of antecedent-hydrological conditions on rainfall triggering of debris flows in ash-fall pyroclastic mantled slopes of Campania (southern Italy). Landslides 13, 967–983.

Onda, Y., Tsujimura, M., Tabuchi, H., 2004. The role of subsurface water flow paths on hillslope hydrological processes, landslides and landform development in steep mountains of Japan. Hydrol. Process. 18, 637–650.

Pagano, L., Picarelli, L., Rianna, G., Urciuoli, G., 2010. A simple numerical procedure for timely prediction of precipitation-induced landslides in unsaturated pyroclastic soils. Landslides 7, 273–289.

Papa, M.N., Medina, V., Ciervo, E., Bateman, A., 2013a. Derivation of critical rainfall thresholds for shallow landslides as a tool for debris flow early warning systems. Hydrol. Earth Syst. Sci. 17, 4095–4107.

Papa, R., Pirone, M., Nicotera, M.V., Urciuoli, G., 2013b. Seasonal groundwater regime in an unsaturated pyroclastic slope. Géotechnique 63 (5), 420–426.

Patacca, E., Scandone, P., 2007. Geological interpretation of the CROP-04 seismic line (Southern Apennines, Italy). In: Mazzotti, A., Patacca, E., Scandone, P. (Eds.), Results of the CROP Project Sub-project CROP-04 Southern Apennines (Italy), Bollettino della Società Geologica Italiana (Italian Journal of Geoscience) Special issue. 7. pp. 297–315.

Pelletier, J.D., Rasmussen, C., 2009. Geomorphically based predictive mapping of soil thickness in upland watersheds. Water Resour. Res. 45 (W09417), 1–15.

Reid, M.E., Nielsen, H.J.P., Dreiss, S.J., 1988. Hydrologic factors triggering a shallow hillslope failure. Bull. Assoc. Eng. Geol. 25 (3), 349–362.

Rolandi, G., Bertollini, F., Cozzolino, G., Esposito, N., Sannino, D., 2000. Sull'origine delle coltri piroclastiche presenti sul versante occidentale del Pizzo D'Alvano (Sarno-Campania). Quaderni di Geologia Applicata 7 (1), 37–47.

Rolandi, G., Maraffi, S., Petrosino, P., Lirer, L., 1993a. The Ottaviano eruption of Somma-Vesuvius (8000 y B.P.): a magmatic alternating fall and flow forming eruption. J. Volcanol. Geotherm. Res. 58, 43–65.

Rolandi, G., Mastrolorenzo, G., Barrella, A.M., Borrelli, A., 1993b. The Avellino Plinian eruption of Somma-Vesuvius (3760 y B.P.): the progressive evolution from magmatic to hydromagmatic style. J. Volcanol. Geotherm. Res. 58, 67–88.

Sidle, R.C., Onda, Y., 2004. Hydrogeomorphology: overview of an emerging science. Hydrol. Process. 18, 597–602.

Sorbino, G., 2005. Numerical modelling of soil suction measurements in pyroclastic soils. In: Cui, Tarantino Romero (Ed.), International Symposium "Advanced Experimental Unsaturated Soil Mechanics". Taylor and Francis Group, London, pp. 541–547.

Stedinger, J.R., Cohn, T., 1986. Flood Frequency Analysis With Historical and Paleoflood Information. Water Resour. Res. 22, 785–793.

Terzaghi, K., 1943. Theoretical Soil Mechanics. John Wiley and Sons. New Yorkpp. 510.

Thornthwaite, C.W., 1948. An Approach toward a Rotational Classification of Climate. Geogr. Rev. 38 (1), 55–94.

Torres, R., Dietrich, W.E., Montgomery, D.R., Anderson, S.P., Loague, K., 1998.

Unsaturated zone processes and the hydrologic response of a steep, unchanneled catchment. Water Resour. Res. 34, 1865–1879.
USDA, 2014. Keys to soil taxonomy. United States Department of Agriculture Natural Resources Conservation Service, 12th ed. (372 pp).
van Genuchten, M.T., 1980. A closed form equation for predicting the hydraulic conductivity of unsaturated soils. Soil Sci. Soc. Am. J. 44, 892–898.
van Genuchten, M.Th., Lesch, S.M., Yates, S.R., 1991. The RETC Code for Quantifying the Hydraulic Functions of Unsaturated Soils. Version 1.0. U.S. Salinity Lab., Riverside, CA.
Varnes, D.J., 1978. Slope movement types and processes. In: Schuster, R.L., Krizek, R.J. (Eds.), Landslides: Analysis and Control Special Report 176. Transportation and Road Research Board, National Academy of Science, Washington D. C., pp. 11–33.
VV.AA, 1990. In: Aderson, M.G., Burt, T.P. (Eds.), Process Studies in Hillslope Hydrology. John Wiley and Sons (550 pp. ISN 0-471-92714-7).
VV.AA, 1996. In: Anderson, M.G., Brooks, M.B. (Eds.), Advances in Hillslope Processes. 1–2. John Wiley and Sons, pp. 1149 (ISBN 0-471-96774-2).
Webb, H.R., Betacourt, J.L., 1992. Climatic Variability and Flood Frequency of the Santa Cruz River, Pima County, Arizona. Geological Survey Water-Supply Paper. 2379. pp. 40.